Geophysical Research Letters

RESEARCH LETTER
10.1029/2020GL087505

Decreasing Landslide Erosion on Steeper Slopes in Soil-Mantled Landscapes

Jeff P. Prancevic[1,2,3], Michael P. Lamb[4], Brian W. McArdell[5], Christian Rickli[5], and James W. Kirchner[1,2,5]

[1]Department of Environmental Systems Science, ETH Zürich, Zürich, Switzerland, [2]Department of Earth and Planetary Science, UC Berkeley, Berkeley, CA, USA, [3]Department of Geography, Planning, and Environment, Concordia University, Montreal, Quebec, Canada, [4]Division of Geological and Planetary Sciences, California Institute of Technology, Pasadena, CA, USA, [5]Swiss Federal Institute for Forest, Snow and Landscape Research WSL, Birmensdorf, Switzerland

Key Points:
- The size and density of rainfall-triggered shallow landslides decrease as slopes steepen beyond the threshold angle for failure
- Steeper slopes have thinner soils that are more easily held in place by cohesion and produce smaller landslides
- Soil creep prevents the accumulation of thick soils on the steepest slopes, inhibiting landslides

Supporting Information:
- Supporting Information S1
- Table S1
- Table S2
- Table S3
- Table S4
- Table S5
- Table S6
- Table S7
- Table S8
- Table S9

Correspondence to:
J. P. Prancevic,
jeff.prancevic@gmail.com

Citation:
Prancevic, J. P., Lamb, M. P., McArdell, B. W., Rickli, C., & Kirchner, J. W. (2020). Decreasing landslide erosion on steeper slopes in soil-mantled landscapes. *Geophysical Research Letters*, *47*, e2020GL087505. https://doi.org/10.1029/2020GL087505

Received 13 FEB 2020
Accepted 20 APR 2020
Accepted article online 3 MAY 2020

Abstract Slope-stability models predict that steeper hillslopes require smaller hydrological triggers for shallow landslides to occur due to the added downslope pull of gravity, which should result in more frequent landslides and faster erosion. However, field observations indicate that landslide frequency does not consistently increase on steeper hillslopes. Here, we use measurements of 1,096 soil landslides in California and Switzerland, and a compilation of landslide geometries, to show that steeper hillslopes typically have thinner soils and that thin soils inhibit landslides due to enhanced roles of cohesion and boundary stresses. We find that the landscape-averaged landslide erosion depth peaks near the threshold slope for instability, and it drops to half that value on hillslopes that are just 5° to 10° steeper. We propose that faster rates of soil creep on steeper slopes cause thin and more stable soils, which in turn reduces landslide erosion, despite the added pull of gravity.

Plain Language Summary Landslides are generally associated with steep terrain, and physics-based models predict that tilting the same soil to steeper angles should increase the likelihood that a landslide is triggered by rainfall. Such predictions are used to assess landslide hazards and model mountain erosion. However, some landslide databases, including two presented here, show that landslides can be equally or less common on steeper slopes. We argue that this discrepancy results from differences in soil thickness. Thin soils are more easily held in place by cohesive forces from plant roots and mineral cohesion, and measurements of soil thickness consistently show that soils tend to be thinner on steeper hillslopes. Not only do thin soils reduce the likelihood of landslide occurrence but they also cause landslides to be smaller, reducing shallow-landslide hazards and erosion on steeper slopes. We present landslide measurements from Switzerland and California that show that shallow-landslide erosion peaks for ~30° hillslopes and rapidly decreases for steeper slopes. These results suggest that soil creep becomes more effective at transporting soil on steeper slopes—thinning soils and inhibiting landslides.

1. Introduction

Rainfall-triggered shallow landslides are dominant agents of soil erosion in many mountainous landscapes (De Rose, 2009; Larsen et al., 2010) and are deadly and costly natural hazards (Schuster & Highland, 2001). These landslides are triggered when stormwater flows through soil and saturates pores, thereby reducing the frictional stability of soils through increased pore pressures (e.g., Taylor, 1948). The critical amount of rainfall that will trigger a landslide varies spatially and depends on a variety of local soil and topographic conditions: upslope contributing drainage area, topographic slope, soil hydraulic conductivity, soil thickness, landslide geometry, soil cohesion (from roots and mineral cohesion), the internal friction angle of the soil, and the direction of seepage flow. Physics-based models for shallow landslide initiation include terms to account for some or all of these factors, but the only terms that can be easily mapped across landscapes are contributing drainage area and topographic slope. Spatial variability in the other parameters is sometimes predicted from topography and classification maps of soil, vegetation, and/or lithology (e.g., Dietrich et al., 1995; Lee & Pradhan, 2007; von Ruette et al., 2013), but these parameters are often treated as constants, and hillslope stability at landscape scales is predicted primarily using drainage area and slope (Kirkby, 1987; Montgomery & Dietrich, 1994; e.g., Benda & Dunne, 1997; Moon et al., 2015).

Models that balance soil friction (reduced by pore-water pressure) with the gravitational force pulling soil downslope can predict the critical water-saturation depth at which landslide failure occurs. Saturation depth can be combined with Darcy flow models to predict the subsurface stormwater discharge required to trigger landslides (termed "triggering discharge" herein). When only hillslope angle is considered, landslide models predict that steeper slopes require smaller triggering discharges for landslides to occur (Dietrich et al., 2001; Montgomery & Dietrich, 1994). Thus, triggering discharges are likely to be exceeded during smaller storm events on steeper slopes (e.g., Iida, 2004), which should cause more frequent landslides there.

Measuring the temporal frequency of landsliding for any given part of a landscape is difficult because landslide recurrence intervals tend to be longer than historical records. However, landslide frequency, and how it varies with slope angle, can be assessed by observing how the spatial density of landsliding varies with slope. Several studies have measured the slope-specific density of landsliding by counting the number of landslides that occurred within a particular range of hillslope angles and dividing that number by the total landscape area within that range. These data sets have revealed a sharp increase in landslide density on steeper slopes for earthquake-triggered landslides (Gorum et al., 2013, 2014; Yamagishi & Iwahashi, 2007), but data sets that include only rainfall-triggered landslides show much weaker relationships (Coe et al., 2004; De Rose, 2013; Marc et al., 2018a; Yamagishi & Iwahashi, 2007), with some landscapes exhibiting the opposite trend—decreasing landslide density on steeper slopes (Gao & Maro, 2010; Korup, 2008).

Decreasing landslide density on steeper slopes might be explained by slope-stability theory if soil properties, stormwater discharge, or landslide geometries adjust to help stabilize soil on steeper slopes. For example, Marc et al. (2018a) suggested that steeper landslide sites might have smaller contributing drainage areas and therefore experience smaller water discharges during a given storm event, but they lacked high-resolution digital elevation models (DEMs) to test this hypothesis. Alternatively, we propose that thinner soils stabilize the soil mantle on steep hillslopes. Cohesion provides a larger stabilizing force relative to gravitational forces for thin slides (De Rose, 2009; Dietrich et al., 1995; Gabet & Dunne, 2002; Parker et al., 2016). In addition, landslides in thinner soils tend to be shorter and narrower (e.g., Larsen et al., 2010), which also helps stabilize hillslopes due to increased boundary stresses (Milledge et al., 2014; Prancevic et al., 2018). Our hypothesis is at odds with previous interpretations that thin soils on steep slopes are a result of landslides more frequently removing the soil mantle (De Rose, 2009; Heimsath et al., 2012). However, studies have yet to directly measure soil thicknesses and landslide density in the same landscape to assess whether thin soils are associated with higher or lower landslide frequency. Here, we explore the idea that landslide activity on steep slopes is actually reduced because of thin soils, rather thin soils being the result of more frequent landsliding.

To test our hypothesis, we use data from 1,096 mapped landslides in California and Switzerland to simultaneously assess the relationship between landslide spatial density, topographic slope, soil thickness, and landslide erosion. We also present a new compilation of landslide geometries, which indicates that soils are consistently thinner on steeper hillslopes (Figure 1) (Barnard et al., 2001; Montgomery, 1991; Morgan et al., 1997; Paudel et al., 2003; Rice et al., 1969; Robison et al., 1999; Van den Eeckhaut et al., 2007; Warburton et al., 2008; Yamagishi & Iwahashi, 2007).

2. Landslide Mapping and Measurement

We examined landslides that were triggered by rainfall in soil-mantled, grassy landscapes in California and Switzerland. A pair of rainfall events triggered 492 landslides in Chino Hills, CA, between 19 and 21 February 2005 (Supporting Information Table S1), and we manually mapped the resulting landslide scars from 60-cm resolution Quickbird orthophotos (Figure 2a). The Swiss data set is composed of separate landslide inventories from eight storm events between 1997 and 2012, with each inventory containing between 25 and 280 landslides (Tables S2–S9). Scars from these landslides were surveyed in the field by the Swiss Federal Institute of Forest, Snow, and Landscape Research (Rickli & Graf, 2009) (e.g., Figures 2b and 2c).

We mapped landslide locations from both regions onto high-resolution lidar DEMs (Figures 2 and S1–S10). Using the DEMs, we measured the topographic gradient and contributing drainage area (using D-infinity flow routing; Tarboton, 1997) for every pixel in the landscape and estimated the values at each landslide location by averaging the 9 pixels surrounding the landslide centroid. Hillslope angles for the Swiss data set were also measured directly in the field using a handheld inclinometer and were similar to the

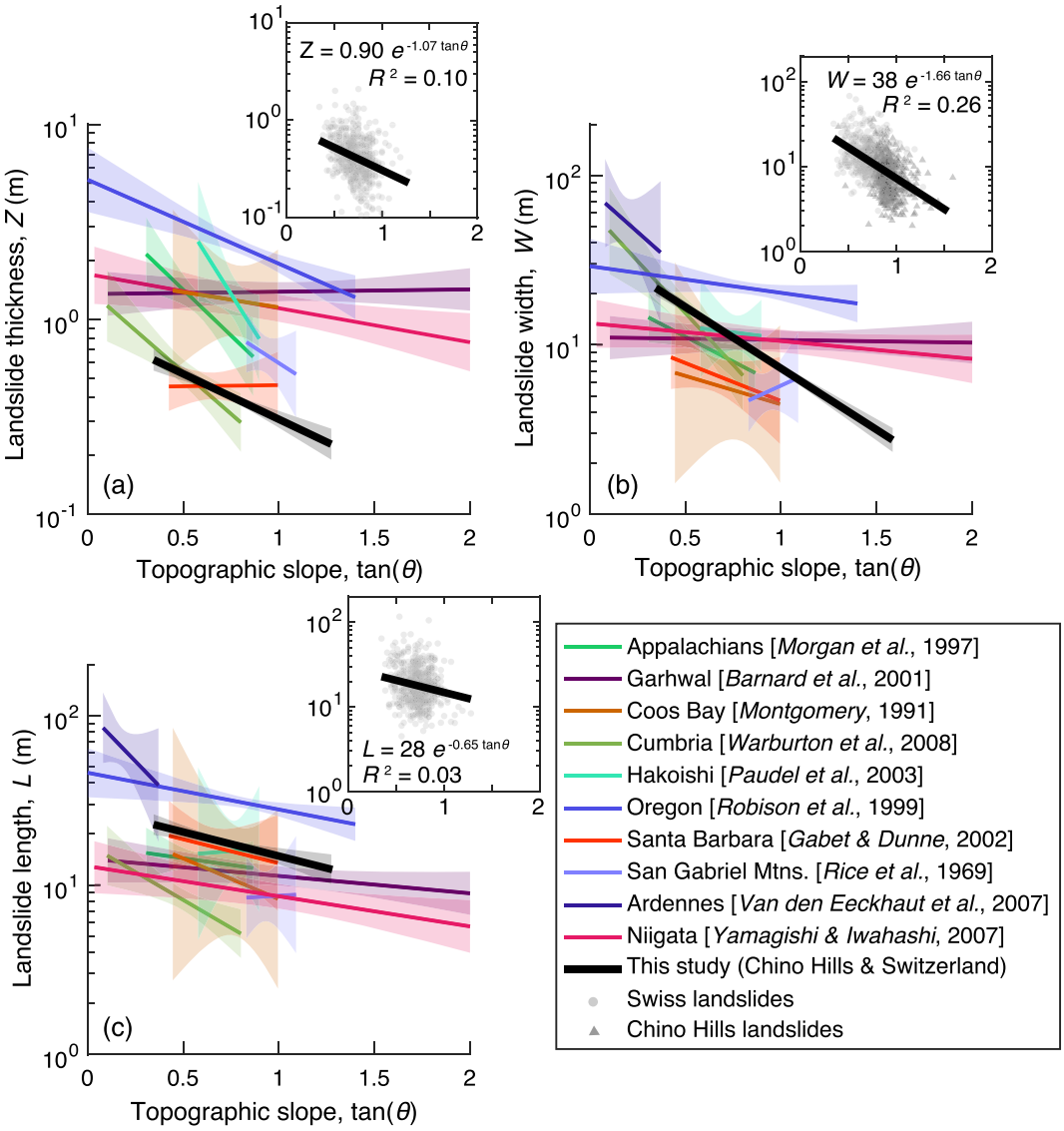

Figure 1. Plots of landslide dimensions: (a) thickness (Z), (b) width (W), and (c) length (L) as functions of topographic slope. Colored lines in the large plots are best-fit regressions of compiled landslide data with 95% confidence bounds shaded around each line. Insets show landslide dimensions for each of the mapped landslides in Switzerland (circles) and Chino Hills (triangles, only width). The black lines in the insets show the best-fit regressions for these landslide measurements and are the same as the black lines in the large plots. Relationships from this study (black lines) are all significant ($p < 10^{-5}$).

DEM-derived values. We estimated the maximum triggering discharge for each landslide by multiplying the contributing drainage area by the maximum 24-hr rainfall rate of the respective storm events (Tables S2–S9). For Chino Hills, we used hourly rain gauge data from a National Oceanic and Atmospheric Administration weather station 7 km southwest of our study area (Coop Station 043285). For the Swiss landslides, we used national daily gridded rainfall data sets that are modeled from interpolated rain gauge data (MeteoSwiss, 2019).

For estimates of landslide sizes, we relied on a combination of field observations, satellite imagery, and landslide scaling relationships. For the Swiss landslides, length (L), width (W), and volume (V) were measured directly in the field, and we used these three measurements to estimate landslide thickness ($D = \frac{V}{LW}$, Tables S2–S9). Most of the landslides had some bedrock exposed at their base, and we therefore assume that the failure plane was at or near the soil-bedrock interface for all mapped landslides, allowing us to estimate soil thickness from landslide geometries. For Chino Hills, we measured the width of each landslide scar from

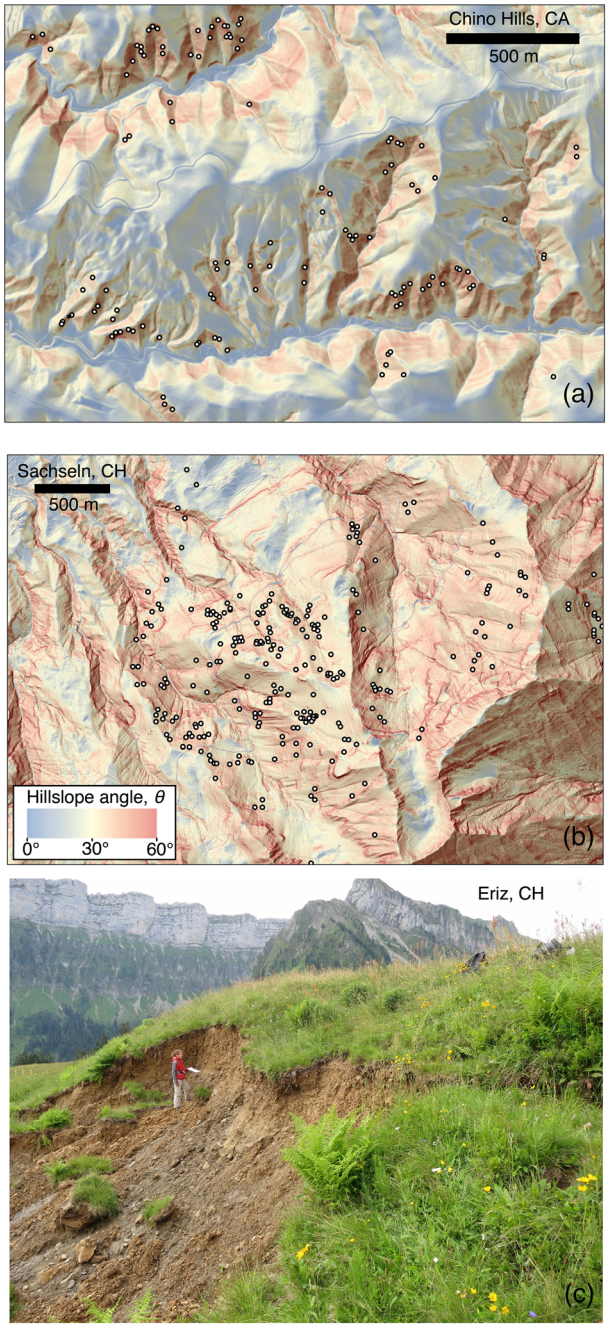

Figure 2. Maps of hillslope angle overlain onto hillshade DEMs for (a) Chino Hills, CA and (b) Sachseln, Switzerland. Mapped shallow landslides are marked with circles. Both maps cover only a subset of the mapped landslides. Full maps are provided in Figures S1-S10. (c) Photograph of a landslide headscarp in Eriz, Switzerland.

satellite imagery; however, landslide length was obscured by runout deposits, and we instead assumed that landslide lengths were twice their widths ($L = 2\ W$) (Frattini & Crosta, 2013; Prancevic et al., 2018) (Table S1). Measurements of landslide thickness were also not available for the Chino Hills data set. Instead, we estimated thicknesses using the best-fit scaling relationship between hillslope angle and landslide/soil thickness that was measured for the Swiss landslides, which were similar to the relationships from the compiled data sets (Figure 1a).

To assess how landslide density and erosion volume change with hillslope angle, we compared the distributions of landslide angles with the total distribution of hillslope angles within the landslide mapping boundaries (Figures S1–S10). The distribution of landslide angles varied considerably between study sites, likely due to differences in soil and vegetation causing differences in soil friction angles and cohesive strength. Therefore, to compare landslide density-slope relationships between sites, we first normalized all hillslope and landslide angles by a threshold angle for each site, θ_{LS10}, defined as the angle above which 90% of the landslides at that site occurred (Figures 3 and 4). We then measured the spatial density of landslides within equally spaced bins of normalized hillslope angle ($\frac{\tan\theta}{\tan\theta_{LS10}}$) by summing the number of landslides and dividing by the total mapping area within each slope bin (Figure 3a). To measure landslide erosion as a function of hillslope angle, we summed the measured landslide volumes and normalized by the total mapping area within each slope bin (Figure 3b). This calculation provided estimates of the average landslide erosion depth—the depth of erosion that would have occurred if the mapped landslides removed a uniform layer of soil from the landscape within that slope bin.

2.1. Model Predictions

We used a force-balance slope-stability model to predict how the triggering discharge is expected to change with topographic slope at our study sites. We modified the three-dimensional model from Milledge et al. (2014) and Prancevic et al. (2018) that balances the downslope weight of pore water and buoyant sediment with frictional and cohesive forces acting on the base, walls, and toe of the landslide (Text S1). This model provides an estimate of the critical soil saturation depths required to trigger landslides and can be used to estimate landslide-triggering discharges (Q_c) when combined with Darcy flow velocities (and overland flow velocities if hillslope soil is oversaturated; Text S1; Prosser et al., 1995). We evaluated the effect of hillslope angle on Q_c with two sets of input variables. In the simplest case, we used constant values for both landslide geometries and soil properties for all slope angles, as is typically done in the absence of detailed landslide and soil measurements. In the second case, we predicted Q_c using slope-dependent landslide dimensions, according to their measured covariance (Figure 1).

3. Results

3.1. Landslide Size and Hillslope Angle

Field measurements of landslide dimensions and volumes in Switzerland revealed that steeper landslides are significantly smaller in all dimensions (Figure 1). In addition, measurements of landslide width in Chino Hills show that landslides were narrower in that landscape, as well. Thus, the volume of sediment mobilized by each landslide decreased on steeper hillslopes at all sites, on average. These trends in landslide geometries

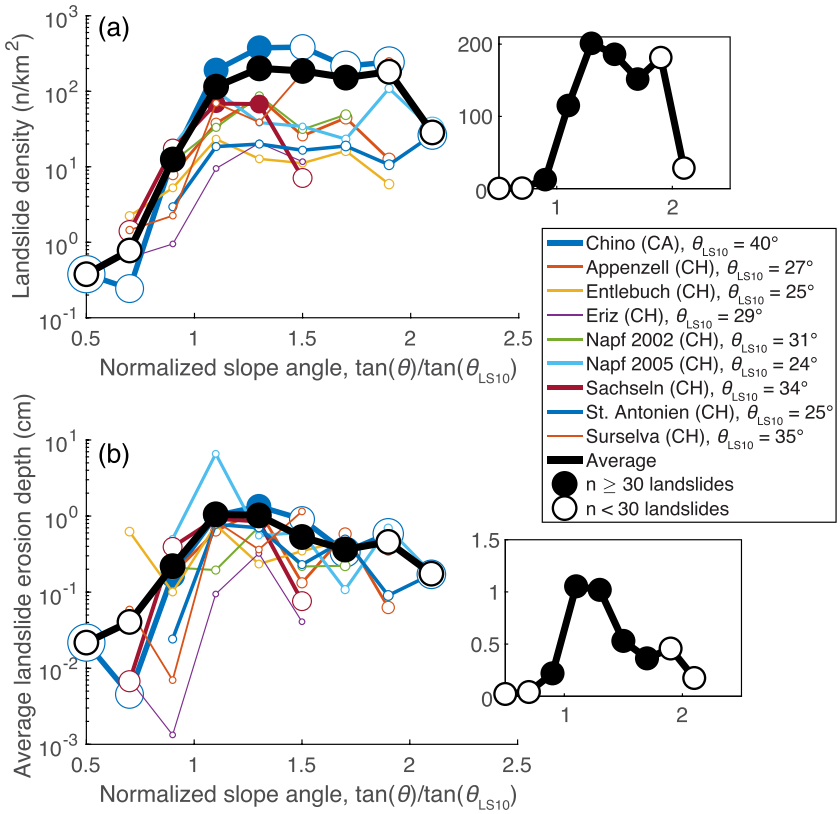

Figure 3. (a) Spatial density of landslides and (b) the average landslide erosion depth as a function of the local slope angle. Line colors correspond to different landslide events/sites, and the thick black line is the average of all events, weighted by the total number of landslides for each event (n). Landslide densities (n/km^2) are the number of landslides within a given slope bin divided by the total landscape area within the slope bin. Average landslide erosion is the total landslide volume mobilized within each slope bin divided by the landscape area within each slope bin. The x axes of both plots were normalized by the threshold slope (θ_{LS10}). Insets in both panels show the data average from the large plots but with linear y axes, showing more clearly an order-of-magnitude decrease in landslide erosion on steeper slopes.

are similar to previous measurements of landslide size (Figure 1), as well as independent measurements of soil thickness (De Rose et al., 1993; Heimsath et al., 2012; Salciarini et al., 2006), indicating that soil thinning on steeper slopes is common globally.

3.2. Landslide Densities and Erosion Depths

The mapped landslides occurred over a broad distribution of slopes. However, at each site, the slope-specific density of landslides increased abruptly at the threshold slope, which ranges from θ_{LS10} = 24° to 40° (Figure 4). On hillslopes steeper than θ_{LS10}, landslide densities for individual landslide events are noisy, but they do not show a general tendency for more landslides on steeper slopes. Instead, when averaged across all of the sites, landslide density remains approximately constant at slopes steeper than the threshold. This is consistent with some previous work on slope-specific landslide density (De Rose, 2013; Gao & Maro, 2010; Korup, 2008; Marc et al., 2018a) and suggests that landslide susceptibility does not monotonically increase with slope, as is often assumed. Moreover, because landslides were smaller on steeper hillslopes, we calculate that average landslide erosion depths decrease sharply at slopes steeper than the threshold angle for landsliding (Figure 3b). For example, when averaged over all sites, the average landslide erosion depth was 1.05 ± 1.02 cm (SD) on hillslopes close to the threshold angle $\left(\frac{\tan\theta}{\tan\theta_{LS10}} = 1.1\right)$, whereas the average landslide erosion depth was 0.50 ± 0.36 cm (SD) on hillslopes that are just 5° to 10° steeper

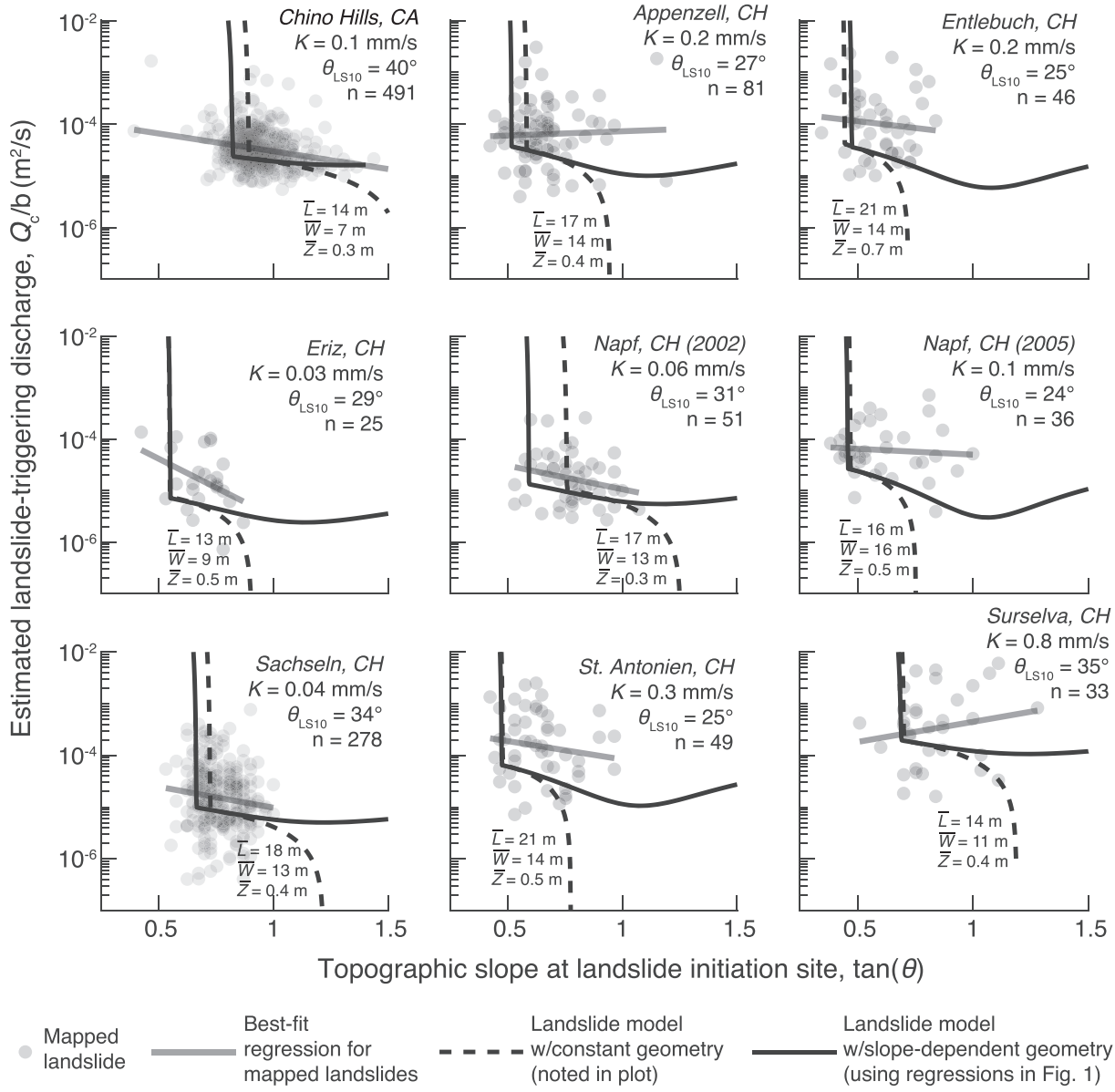

Figure 4. Maximum estimates of the width-specific landslide-triggering discharge (drainage area times the maximum hourly rainfall divided by DEM cell size, b) as a function of topographic slope for landslides at each study site. The semitransparent gray dots are data for individual landslides. Best-fit regressions (exponential) are shown as gray lines. None of these relationships are statistically significant ($p > 0.01$). The black lines in each panel are the 3-D force-balance model predictions (Text S1) assuming constant landslide geometries (dashed) and allowing landslide geometries to vary with slope using the regressions in Figure 1 (solid). Site-specific parameters that were used in both model predictions are listed in each panel. The hydraulic conductivity, K, was tuned to match the y-axis positions of the data and models, the bulk friction angle of soil was assumed to equal the threshold slope, $\phi = \theta_{LS10}$, and characteristic landslide dimensions were estimated by taking the average of measured or estimated dimensions. We used constant values for other model input parameters for which we have no estimates: total cohesion, $C = 2.2$ kPa, and soil porosity, $\eta = 0.3$.

$\left(\frac{\tan\theta}{\tan\theta_{LS10}} = 1.5\right)$. In other words, in these mapped events, landslides were twice as erosive on hillslopes near the threshold angle than on hillslopes that were just 10° steeper.

3.3. Landslide-Triggering Discharges

Estimates of landslide-triggering stormwater discharges vary by orders of magnitude at each site but are not significantly correlated with hillslope angle at any of the field sites ($p > 0.01$; Figure 4). Thus, hillslope angle

is not a good predictor of how much water was required to trigger these landslides, and, on average, landslides at all hillslope angles occurred with similar triggering discharges. In contrast, our force-balance slope-stability model predicts a sharp decrease in triggering discharge at steeper slopes, assuming all other variables remain constant (Figure 4). This comparison suggests that observed landslide densities (Figure 3a) cannot be explained solely by steeper slopes experiencing smaller triggering discharges (Marc et al., 2018a) and that other soil or landslide properties must covary with slope to explain the data.

Instead of assuming a constant landslide geometry, we next evaluated how observed changes in soil thickness and landslide dimensions with hillslope angle affect soil stability. By using slope-dependent geometries (Figure 1), our slope stability model predicts that Q_c is relatively constant for slopes greater than $\tan\theta_{LS10}$, making it more consistent with estimates of triggering discharge for the observed landslides (Figure 4). This result suggests that thinner soils and smaller landslide dimensions—which reduce the weight of the wet soil that must be supported by cohesion and boundary friction—help explain the tendency for the triggering discharge to remain approximately constant on slopes steeper than the threshold angle.

4. Discussion

4.1. The Influence of Soil Accumulation on Landslide Susceptibility and Erosion Rates

At our study sites, very steep hillslopes produced a similar density of landslides as hillslopes close to the threshold angle. The landslides that did occur on slopes much steeper than the threshold angle tended to be smaller in all dimensions, meaning that the fraction of the landscape covered by landslide scars was smaller on the steepest hillslopes than those near the threshold angle. If we assume that these patterns of landslide size and density are representative of long-term averages over several landsliding cycles, our results suggest that landslide frequency peaks near the threshold angle and then decreases on steeper slopes. Therefore, on steeper slopes, more time elapses between successive landslides and less soil accumulates during those longer periods based on observations of landslide thickness (Figure 1a). Thus, the average rate of soil accumulation between landslides must be slower on steeper slopes. This is in contrast to previous studies that concluded that soils are thinner on steeper slopes because landslides remove soil from those hillslopes more frequently (De Rose, 2009; Heimsath et al., 2012). Because the intuitive assumption that landslide frequency increases on steeper slopes does not hold at our sites, there must be another mechanism to explain the thin soils found there.

The slow rate of soil accumulation could reflect either slower rates of local soil production or greater net loss of soil through diffusive soil transport. Local variability in soil production rates is thought to depend primarily on local soil thickness and not directly on topography (e.g., Heimsath et al., 1997). Because steeper hillslopes tend to have thinner soils (e.g., Figure 1), a depth-dependent soil production function implies that soil production rates should be faster on steeper hillslopes and are thus unlikely to explain slow rates of soil accumulation there. However, steeper hillslopes also tend to have faster rates of soil creep and can therefore evacuate locally produced soil more quickly without en masse landslide failures (e.g., Heimsath et al., 1997; Roering et al., 1999). Steeper hillslope angles are also thought to be less effective at trapping and accumulating incoming sediment particles from upslope (e.g., Dibiase et al., 2017; Foufoula-Georgiou et al., 2010; Furbish & Roering, 2013). We therefore conclude that soil transport processes become more efficient on steeper slopes, causing thinner soils and less frequent shallow landslides.

Although we focused our analysis on soil thickness, it is possible that cohesion, hydraulic conductivity, and soil friction angle vary systematically with hillslope angle as well; these properties could also influence landslide occurrence, but we lack measurements of these soil properties to assess this possibility. Our results are also limited to soil landslides. While soil thickness affects stability along the soil-bedrock interface, it is likely negligible for landslides that fail in the underlying bedrock. Consequently, without the stabilizing effect of thin soils, it is possible that bedrock landslides increase in size and frequency on steeper hillslopes. Previous attempts to measure the slope-dependence of landscape frequency have found a wide range of behaviors, and this range might be due to having a mixture of bedrock and soil landslides in their databases (Clarke & Burbank, 2010; Coe et al., 2004; De Rose, 2013; Gorum et al., 2013, 2014; Korup, 2008; Larsen & Montgomery, 2012; Marc et al., 2018b).

4.2. Implications for Landslide Hazards

Our results imply that rainfall-triggered shallow-landslide risk on the steepest hillslopes may be overpredicted if variability in soil thickness is not considered. There are several ways that changes in soil thickness could be included, directly or indirectly, in landslide modeling or hazard assessment (Federal Office for the Environment, 2016). In one approach, soil thickness can be predicted from topography using models for soil production and diffusive soil transport (Dietrich et al., 1995; von Ruette et al., 2013). In another approach, Salciarini et al. (2006) estimated soil thickness as a function of hillslope angle (e.g., Figure 1). Our results show that the effects of soil thinning on steeper hillslopes can offset the increased pull of gravity there, making hillslope angle alone a poor predictor of both shallow-landslide probability and triggering conditions on hillslopes steeper than the threshold angle (Figures 3 and 4).

5. Conclusions

We analyzed two data sets of rainfall-triggered landslides in soil-mantled landscapes—in Chino Hills, California and the Swiss Prealps—to test for the effect of topographic slope on landslide spatial density and size. Data from these sites and from previous studies indicate that landslides tend to be smaller in all dimensions on steeper hillslopes (Figure 1). Moreover, we found that landslide densities peaked close to the lowest slope angle where landslides occurred (the threshold slope) and then were approximately constant on steeper hillslopes (Figure 3a). Combining trends in landslide volume and density, we found that the average landslide erosion depth decreased for steeper hillslope angles beyond the threshold angle for failure (Figure 3b). We also used contributing drainage area to estimate the water discharge required to trigger each landslide and found that discharges were not correlated with hillslope angle. These results are inconsistent with slope stability models that assume uniform soil thickness and are more consistent with models that consider the impact of thinner soils on steeper hillslopes (Figure 4). Rather than enhanced landsliding causing thin soils on steep slopes, as suggested previously, we propose that faster rates of soil creep and particle transport reduce soil thicknesses on steeper slopes, making the soil mantle more stable and landslides smaller. Consequently, for rainfall-triggered slides in soil, erosion and hazards can be smaller on steeper hillslopes.

Acknowledgments
J. P. P. was funded by Uniscientia Stiftung, the ETH Foundation, and SNF grant P400P2_183929. The authors thank Isaac Larsen and David Milledge for providing the landslide geometry compilations that are shown in Figure 1. All data used to make the figures are available at https://www.hydroshare.org/resource/037197c2aaa24aeaa18f4e6e1fe5be4a/. Additional data from the Swiss landslides not used in this publication is freely available here: https://hangmuren.wsl.ch/index.html.

References

Barnard, P., Owen, L. A., Sharma, M. C., & Finkel, R. C. (2001). Natural and human-induced landsliding in the Garhwal Himalaya of northern India. *Geomorphology*, *40*(1–2), 21–35. https://doi.org/10.1016/S0169-555X(01)00035-6

Benda, L., & Dunne, T. (1997). Stochastic forcing of sediment supply to channel networks from landsliding and debris flow. *Water Resources Research*, *33*(12), 2849–2863. https://doi.org/10.1029/97WR02388

Clarke, B. A., & Burbank, D. W. (2010). Bedrock fracturing, threshold hillslopes, and limits to the magnitude of bedrock landslides. *Earth and Planetary Science Letters*, *297*(3–4), 577–586. https://doi.org/10.1016/j.epsl.2010.07.011

Coe, J. A., Michael, J. A., Crovelli, R. A., Savage, W. Z., LaPrade, W. T., & Nashem, W. D. (2004). Probabilistic assessment of precipitation-triggered landslides using historical records of landslide occurrence, Seattle, Washington. *Environmental and Engineering Geoscience*, *10*(2), 103–122. https://doi.org/10.2113/10.2.103

De Rose, R. C. (2009). Quantifying sediment production in steepland environments. *Eurasian Journal of Forest Research*, *12*(1), 9–46.

De Rose, R. C. (2013). Slope control on the frequency distribution of shallow landslides and associated soil properties, North Island, New Zealand. *Earth Surface Processes and Landforms*, *38*(4), 356–371. https://doi.org/10.1002/esp.3283

De Rose, R. C., Trustrum, N. A., & Blaschke, P. M. (1993). Post-deforestation soil loss from steepland hillslopes in Taranaki, New Zealand. *Earth Surface Processes and Landforms*, *18*(2), 131–144. https://doi.org/10.1002/esp.3290180205

Dibiase, R. A., Lamb, M. P., Ganti, V., & Booth, A. M. (2017). Slope, grain size, and roughness controls on dry sediment transport and storage on steep hillslopes. *Journal of Geophysical Research: Earth Surface*, *122*, 941–960. https://doi.org/10.1002/2016JF003970

Dietrich, W. E., D. Bellugi, and R. de Real Asua (2001), Validation of the Shallow Landslide Model, SHALSTAB, for Forest Management, in *Land Use and Watersheds Human Influence on Hydrology and Geomorphology in Urban and Forest Areas, Water Science and Application*, vol. 2, pp. 195–227, Land use and.

Dietrich, W. E., Reiss, R., Hsu, M. L., & Montgomery, D. R. (1995). A process-based model for colluvial soil depth and shallow landsliding using digital elevation data. *Hydrological Processes*, *9*(3–4), 383–400. https://doi.org/10.1002/hyp.3360090311

Federal Office for the Environment (2016). Protection against mass movement hazards, Federal Office for the Environment, Bern. The environment in practice.

Foufoula-Georgiou, E., Ganti, V., & Dietrich, W. E. (2010). A nonlocal theory of sediment transport on hillslopes. *Journal of Geophysical Research*, *115*, F00A16. https://doi.org/10.1029/2009JF001280

Frattini, P., & Crosta, G. B. (2013). The role of material properties and landscape morphology on landslide size distributions. *Earth and Planetary Science Letters*, *361*, 310–319. https://doi.org/10.1016/j.epsl.2012.10.029

Furbish, D. J., & Roering, J. J. (2013). Sediment disentrainment and the concept of local versus nonlocal transport on hillslopes. *Journal of Geophysical Research: Earth Surface*, *118*, 937–952. https://doi.org/10.1002/jgrf.20071

Gabet, E. J., & Dunne, T. (2002). Landslides on coastal sage-scrub and grassland hillslopes in a severe El Niño winter: The effects of vegetation conversion on sediment delivery. *Geological Society of America Bulletin*, *114*(8), 983–990. https://doi.org/10.1130/0016-7606(2002)114<0983:LOCSSA>2.0.CO;2

Gao, J., & Maro, J. (2010). Topographic controls on evolution of shallow landslides in pastoral Wairarapa, New Zealand, 1979–2003. *Geomorphology*, *114*(3), 373–381. https://doi.org/10.1016/j.geomorph.2009.08.002

Gorum, T., Korup, O., van Westen, C. J., van der Meijde, M., Xu, C., & van der Meer, F. D. (2014). Why so few? Landslides triggered by the 2002 Denali earthquake, Alaska. *Quaternary Science Reviews*, *95*, 80–94. https://doi.org/10.1016/j.quascirev.2014.04.032

Gorum, T., van Westen, C. J., Korup, O., van der Meijde, M., Fan, X., & van der Meer, F. D. (2013). Complex rupture mechanism and topography control symmetry of mass-wasting pattern, 2010 Haiti earthquake. *Geomorphology*, *184*, 127–138. https://doi.org/10.1016/j.geomorph.2012.11.027

Heimsath, A., Dietrich, W., Nishiizumi, K., & Finkel, R. (1997). The soil production function and landscape equilibrium. *Nature*, *388*(6640), 358–361.

Heimsath, A. M., Dibiase, R. A., & Whipple, K. X. (2012). Soil production limits and the transition to bedrock-dominated landscapes. *Nature Geoscience*, *5*(3), 210–214. https://doi.org/10.1038/ngeo1380

Iida, T. (2004). Theoretical research on the relationship between return period of rainfall and shallow landslides. *Hydrological Processes*, *18*(4), 739–756. https://doi.org/10.1002/hyp.1264

Kirkby, M. J. (1987). Modelling some influences of soil erosion, landslides and valley gradient on drainage density and hollow development. In F. Ahnert, & W. Cremlingen (Eds.), *Geomorphological models theoretical and empirical aspects* (Vol. 10, pp. 1–14). Germany: Catena.

Korup, O. (2008). Rock type leaves topographic signature in landslide-dominated mountain ranges. *Geophysical Research Letters*, *35*, L11402. https://doi.org/10.1029/2008GL034157

Larsen, I. J., & Montgomery, D. R. (2012). Landslide erosion coupled to tectonics and river incision. *Nature Geoscience*, *5*(7), 468–473. https://doi.org/10.1038/ngeo1479

Larsen, I. J., Montgomery, D. R., & Korup, O. (2010). Landslide erosion controlled by hillslope material. *Nature Geoscience*, *3*(4), 247–251. https://doi.org/10.1038/ngeo776

Lee, S., & Pradhan, B. (2007). Landslide hazard mapping at Selangor, Malaysia using frequency ratio and logistic regression models. *Landslides*, *4*(1), 33–41. https://doi.org/10.1007/s10346-006-0047-y

Marc, O., Stumpf, A., Malet, J.-P., Gosset, M., Uchida, T., & Chiang, S.-H. (2018a). Initial insights from a global database of rainfall-induced landslide inventories: The weak influence of slope and strong influence of total storm rainfall. *Earth Surface Dynamics*, *6*(4), 903–922. https://doi.org/10.5194/esurf-6-903-2018

Marc, O., Stumpf, A., Malet, J.-P., Gosset, M., Uchida, T., & Chiang, S.-H. (2018b). Towards a global database of rainfall-induced landslide inventories: First insights from past and new events. *Earth Surface Dynamics*, *1–28*. https://doi.org/10.5194/esurf-2018-20

MeteoSwiss (2019), MeteoSwiss spatial climate analyses: Documentation of datasets for users, Swiss Federal Office of Meteorology and Climatology.

Milledge, D. G., Bellugi, D., McKean, J. A., Densmore, A. L., & Dietrich, W. E. (2014). A multidimensional stability model for predicting shallow landslide size and shape across landscapes. *Journal of Geophysical Research: Earth Surface*, *119*, 2481–2504. https://doi.org/10.1002/2014JF003135

Montgomery, D., & Dietrich, W. (1994). A physically-based model for the topographic control on shallow landsliding. *Water Resources Research*, *30*(4), 1153–1171.

Montgomery, D. R. (1991), Channel initiation and landscape evolution, UC Berkeley.

>Moon, S., Shelef, E., & Hilley, G. E. (2015). Recent topographic evolution and erosion of the deglaciated Washington cascades inferred from a stochastic landscape evolution model. *Journal of Geophysical Research: Earth Surface*, *120*, 856–876. https://doi.org/10.1002/2014JF003387

Morgan, B. A., G. F. Wieczorek, R. H. Campbell, and P. L. Gori (1997), Debris-flow hazards in areas affected by the June 27, 1995, storm in Madison County, Virginia, *USGS Open-File Report*, (97–438), 1–33, doi:https://doi.org/10.3133/ofr97438.

Parker, R. N., Hales, T. C., Mudd, S. M., Grieve, S. W. D., & Constantine, J. A. (2016). Colluvium supply in humid regions limits the frequency of storm-triggered landslides. *Scientific Reports*, *6*(1), 34438. https://doi.org/10.1038/srep34438

Paudel, P. P., Moriwaki, K., Morita, K., Kubota, T., & Omura, H. (2003). An assessment of shallow landslides mechanism induced by rainfall in Hakoishi area. *Kyushu Journal of Forest Research*, *56*(3), 122–128.

Prancevic, J. P., Lamb, M. P., Palucis, M. C., & Venditti, J. G. (2018). The role of three-dimensional boundary stresses in limiting the occurrence and size of experimental landslides. *Journal of Geophysical Research: Earth Surface*, *123*, 46–65. https://doi.org/10.1002/2017JF004410

Prosser, I. P., Dietrich, W. E., & Stevenson, J. (1995). Flow resistance and sediment transport by concentrated overland-flow in a Grassland Valley. *Geomorphology*, *13*(1–4), 71–86. https://doi.org/10.1016/0169-555X(95)00020-6

Rice, R. M., Crobett, E. S., & Bailey, R. G. (1969). Soil slips related to vegetation, topography, and soil in Southern California. *Water Resources Research*, *5*(3), 647–659. https://doi.org/10.1029/WR005i003p00647

Rickli, C., & Graf, F. (2009). Effects of forests on shallow landslides–Case studies in Switzerland. *Forest Snow and Landscape Research*, *82*(1), 33–44.

Robison, E. G., K. A. Mills, J. Paul, L. Dent, and A. Skaugset (1999), Oregon Department of Forestry Storm Impacts and Landslides of 1996: Final report.

Roering, J. J., Kirchner, J. W., & Dietrich, W. E. (1999). Evidence for nonlinear, diffusive sediment transport on hillslopes and implications for landscape morphology. *Water Resources Research*, *35*(3), 853–870. https://doi.org/10.1029/1998WR900090

Salciarini, D., Godt, J. W., Savage, W. Z., Conversini, P., Baum, R. L., & Michael, J. A. (2006). Modeling regional initiation of rainfall-induced shallow landslides in the eastern Umbria Region of central Italy. *Landslides*, *3*(3), 181–194. https://doi.org/10.1007/s10346-006-0037-0

Schuster, R. L., and L. M. Highland (2001), Socioeconomic and environmental impacts of landslides in the western hemisphere, U.S. Geological Survey.

Tarboton, D. G. (1997). A new method for the determination of flow directions and upslope areas in grid digital elevation model. *Water Resources Research*, *33*(2), 309–319.

Taylor, D. W. (1948). *Fundamentals of soil mechanics*. New York, NY: John Wiley & Sons.

Van den Eeckhaut, M., Poesen, J., Govers, G., Verstraeten, G., & Demoulin, A. (2007). Characteristics of the size distribution of recent and historical landslides in a populated hilly region. *Earth and Planetary Science Letters*, *256*(3–4), 588–603. https://doi.org/10.1016/j.epsl.2007.01.040

von Ruette, J., Lehmann, P., & Or, D. (2013). Rainfall-triggered shallow landslides at catchment scale: Threshold mechanics-based modeling for abruptness and localization. *Water Resources Research*, *49*, 6266–6285. https://doi.org/10.1002/wrcr.20418

Warburton, J., Milledge, D. G., & Johnson, R. (2008). Assessment of shallow landslide activity following the January 2005 storm, Northern Cumbria. *Cumberland Geological Society Proceedings*, *8*(1), 263–283.

Yamagishi, H., & Iwahashi, J. (2007). Comparison between the two triggered landslides in mid-Niigata, Japan by July 13 heavy rainfall and October 23 intensive earthquakes in 2004. *Landslides*, *4*(4), 389–397. https://doi.org/10.1007/s10346-007-0093-0